Fourth International Meeting on Wind Turbine Noise

Rome Italy 11-14 April 2011

Microseismic Noise from Wind Turbines in the vicinity of the Virgo Gravitational Wave Detector

I. Fiori (1), G. Saccorotti (2), D. Piccinini (2), L. Cauchie (2,3) and F. Paoletti (1,4)

(1) European Gravitational Observatory, Cascina, Pisa (Italy)
(2) Istituto Nazionale di Geofisica e Vulcanologia, Pisa (Italy)
(3) University College of Dublin, School of Geological Sciences, Dublin(Ireland)
(4) Istituto Nazionale di Fisica Nucleare, Pisa (Italy).

irene.fiori@ego-gw.it

Abstract

Soil vibrations produced by wind turbines are a possible concern for scientific experiments performing extremely accurate length measurement; such as the Virgo gravitational wave detector (Cascina, Pisa, Italy). We present the case study of the seismic disturbance produced by a wind park of four 2MW turbines located at a few km from Virgo. The site seismic wave-field has been studied by means of seismic array measurements and correlations with wind speed, which permitted to disentangle the seismic signal of the wind park from the anthropogenic noise background. The main seismic component is found at 1.7Hz and its spectral amplitude is measured to be still above the quiet noise background at distances of 11km from the park. A model is proposed which explains the measured attenuation properties accounting for the site geology. Separately we also find a relationship between wind speed and seismic amplitude. These two pieces of information are used to asses a predictive relationship linking wind speeds with expected seismic noise amplitude for any custom configuration of turbines.

1. Virgo and its seismic issue

Virgo is a large laser interferometer aiming to the detection of the tiny space deformations associated to Gravitational Waves, which according to Einstein's theory of general relativity, are produced by large accelerated masses like Supernovae explosions, spinning neutron stars or coalesce of binary star systems [Saulson, 1].

Virgo is hosted by the European Gravitational Observatory (EGO) which is a French-Italian (CNRS and INFN) scientific consortium. EGO-Virgo is located about 15km South-East of the city of Pisa, Italy. Figure 1 shows a map of the area. The site is within the Arno river alluvial basin; it is bounded by the Monti Pisani to the North, another smooth relief to the South, and the Tyrrhenian Sea to the West. The geology of the area is well documented by several borehole explorations and stratigraphy studies [Cantini,2] also performed during Virgo construction [Stefanelli,3] as consisting of shallow lime sediments up to a depth of 50m, followed by gravel deposits, and a layer of carbonate bedrocks at a depth of about 800m.

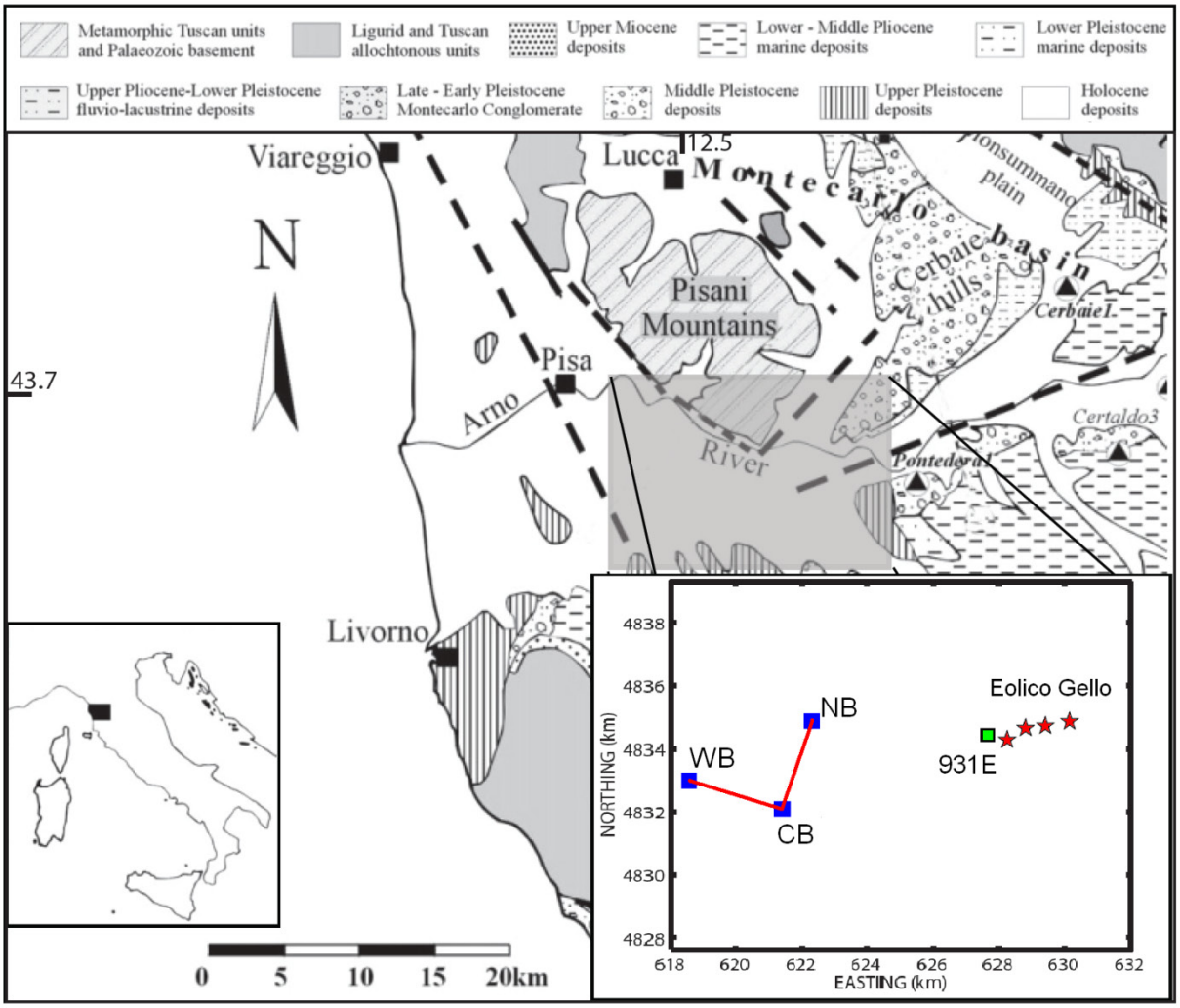

Figure 1 – Simplified geological map of central-western Tuscany including the study area (shaded rectangle). The inset at the bottom right shows the layout of Virgo with positions of the Virgo Central Building (CB), West Building (WB) and North Building (NB); the location of the four turbines (red stars) of the existing wind park named “Eolico Gello”, and the position of seismic station 931E (instrumented with one Lennartz Le3D-5s) which was kept fixed in continuous acquisition during the whole measurement campaign.

Virgo is a Michelson interferometer made of two 3km long perpendicular arms [The Virgo collaboration, 4]. A laser light beam is split in two by one semi-reflective mirror placed at the arms common vertex, and reflected back by mirrors placed at the arms extremities. An impinging GW is expected to alternatively stretch one arm while compressing the other. By reading the phase shift of the recombined beam an extremely precise measurement of the arm length difference is made. Virgo is sensible to strain variations of the order of 10^{-22} in the range from 10Hz to 10000Hz. To obtain this performance Virgo exploits frontier technologies in the field of ultra-stable high power lasers, super-polished mirrors, ultra-high vacuum, and extremely efficient seismic isolation [Accadia, 5]. Nevertheless, intense low-frequency ground vibrations might overcome the seismic isolation systems and deteriorate the Virgo performance. One concern is that 0.1-10Hz monochromatic ground vibrations can match and excite the resonant modes of the Virgo isolation systems. Another concern is the phenomenon of diffused light [Accadia, 6]. Tiny fractions of the light beam might, because of mirrors imperfections, get off the main beam path, hit ground-connected parts and be scattered back-in carrying a phase noise which has "memory" of the scatterer vibration. To illustrate the relevance of this noise path, Figure 2 shows the expected impact of an increase of a factor 10 of the RMS ground seism in the 1Hz to 2Hz frequency range. The associated strain noise would be limiting the sensitivity of the present Virgo and its upgraded version ("Advanced Virgo" foreseen for operation in 2015).

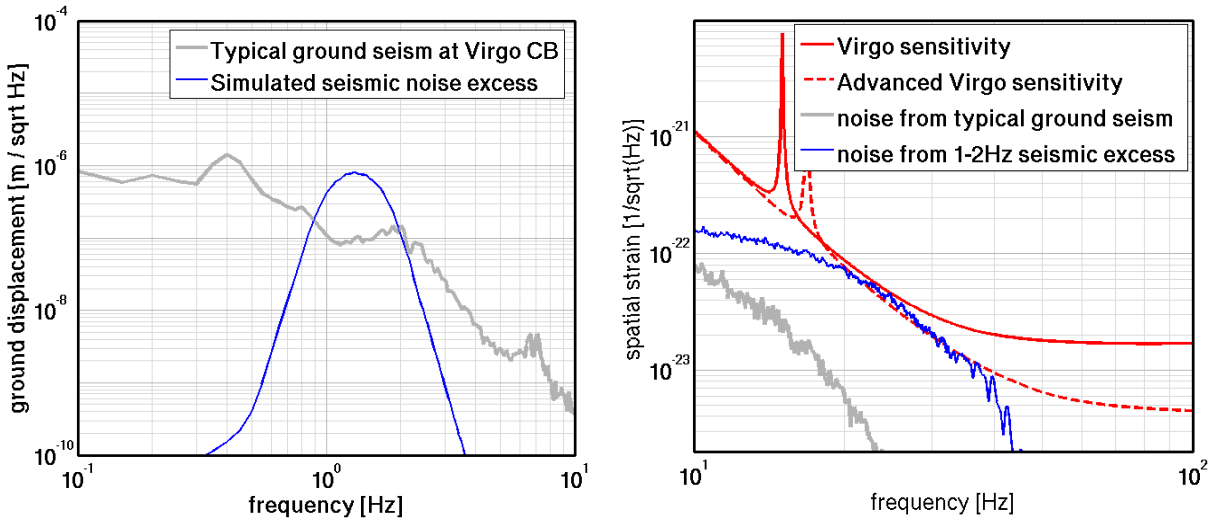

Figure 2 – Predicted impact on Virgo of an increased ground seism at 1-2Hz. Left: ground displacement due to normal seism (grey) and simulated excess in the 1-2Hz region (blue). Right: projected noise in the Virgo Gravitational Wave signal associated to the typical ground seism (grey) and the excess seism (blue). The projection is done using the diffused light noise model described in [Accadia, 6] and a typical noise coupling value (G=1E-21) measured in Virgo. Note the diffused light noise model is not linear: a ground displacement noise at a few Hz causes a noise at 10-50Hz in the Virgo output signal.

Wind Turbines (WT) are known to emit acoustic and seismic noise which might still be detected at far distances [Schofield, 7; Styles, 8].

In the previous edition of this conference (WTN2009) we reported about the concern for the possible disturbance produced by a wind farm planned for construction in the vicinity of Virgo. In that occasion we illustrated results of seismic measurements at one wind farm in Germany, and used that data to extrapolate possible effects at Virgo [Fiori, 9].

The wind farm is now in operation: “Eolico Gello” consists of four 2MW turbines of 3-bladed type located East of Virgo. The closest turbine is at 5.9 km from the far extremity of the Virgo North arm. Also, additional turbines are proposed for installation in the vicinity of the EGO site. These are: an extension of “Eolico Gello” with the addition of 3 turbines, and a new wind farm (named “Guasticce”) counting six turbines located South-West of Virgo. Figure 3 illustrates the present and proposed wind parks layout.

EGO has commissioned to the Italian Institute of Geophysics and Volcanology (*Istituto Nazionale di Geofisica e Vulcanologia*, *INGV*) a noise study aimed at verifying properties and intensity of the vibrations produced by the existing wind turbines and assessing the possible impact of the new proposed wind farms. Details of this study are given in one article which has been recently accepted for publication [Saccorotti, 10]. Here we report the main results of this study. In Section 2 we describe the measurements; in Section 3 we describe how the wind park seismic signal has been disentangled from the anthropogenic noise by correlating it with wind and by measuring its directional properties; in Section 4 we describe the attenuation measurement and its modeling; in Section 5 we propose a predictive model which we apply to the new wind park projects.

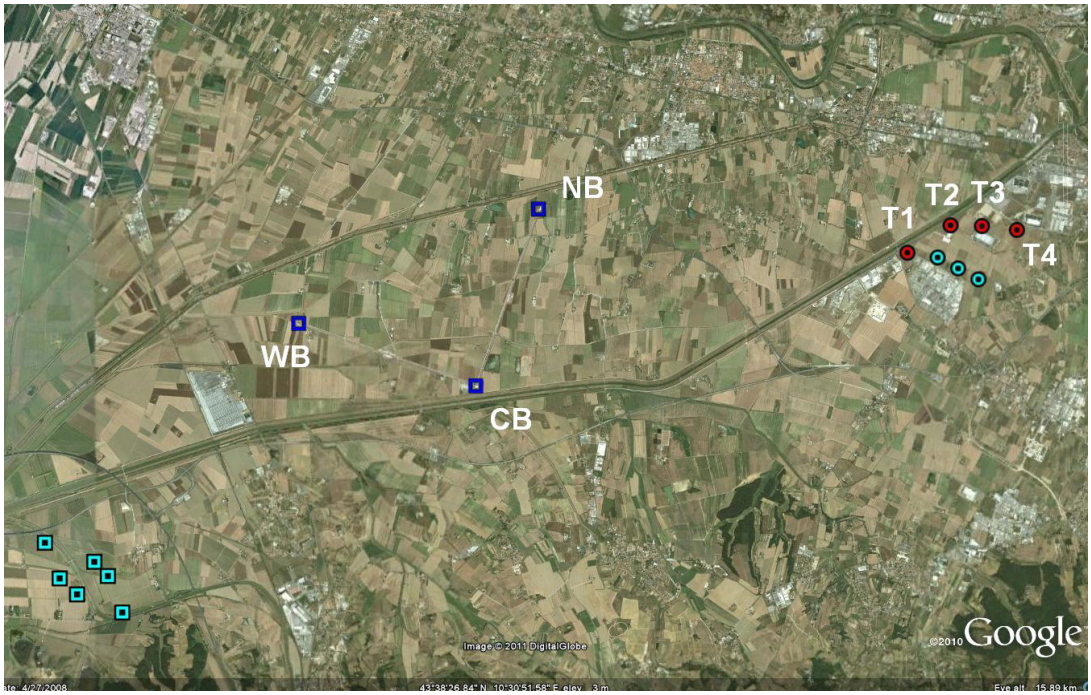

Figure 3 – Map of the study area. It is shown Virgo’s West Building-WB, North Building-NB and Central Building-CB), the existing “Eolico Gello” wind park (red circles: T1 to T4), its proposed extension (light-blue circles) and the proposed new wind park “Guasticce” (light-blue squares in the bottom left).

2. Acquisition of seismic data

The measurement campaign was carried out between October 26 and November 17 2009. This period covers a wide range of wind conditions also encompassing periods of intense winds. A total of 17 seismic stations was employed, six of which were kept in fixed position through the whole campaign duration, while the others were arranged in different size and aperture array geometries for short duration measurements of wave-field directional and attenuation properties. Sensors consisted of Lennartz LE3D-5s velocimeters (flat response bandwidth 0.2-40Hz), Guralp CMG-40T tri-axial velocimeters (0.025-50Hz) and EpiSensors FBA ES-T tri-axial accelerometers (0.1-100Hz). Instruments were calibrated and cross calibrated before the beginning of the survey. Along the data collection period, each individual recorder performed hourly synchronizations to the Global Positioning System time signal. Throughout the study period wind speed and direction was measured by one anemometer (Davis, Vantage Pro ISS) located atop of the Virgo control building at about 10m from soil.

3. Identification of the Wind Turbine seismic wave field

3.1 Measurement with a single station

The time-frequency plot in Figure 4 illustrates the measured characteristics of frequency and time variability of the soil seismic noise amplitude at about 1200m W of the west-most turbine through the entire duration of the study campaign (station "931E" in Figure 1).

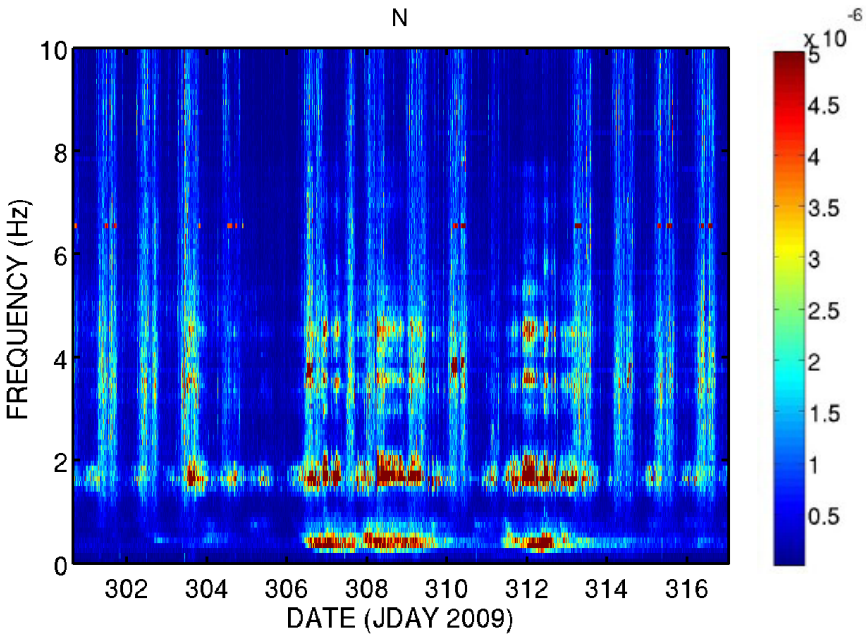

Figure 4 – Spectrogram for the horizontal (N) component of motion at station 931E for the whole duration of the survey. Each column in the plot is the spectral amplitude estimated by averaging 10 discrete Fourier transforms over subsequent not-overlapping 60-s-long windows of signal. Colour scale unit is $ms^{-1}/\sqrt{Hz}$. The time scale is expressed in Julian days from the beginning of the year; as a reference, day 302 corresponds to October 29 2009.

The site seismicity over the 1 to 20Hz range evidences a typical daily periodicity with maxima at working hours and minima at night time and weekends. In order to investigate the noise components likely due to the WTs, we investigated the correlation between noise amplitude and wind speed. The rows of the spectrogram in Figure 4 are time series of spectral amplitude which we average over 0.1Hz-wide frequency bins and we cross correlate against the contemporaneous time series of wind speed. In Figure 5 the maxima of the correlation function and the associated time lag (i.e. the delay between an increase of seismic noise and a correlated increase of wind speed) is plotted against the bins central frequency. Correlation is markedly good at some peculiar frequencies: 0.45Hz, 1.7Hz, 3.5Hz and 4.5Hz. Among these, only the 0.45Hz seism correlates with a delay of some hundreds minutes. This evidence points to a different origin of the 0.45Hz seism which might be marine microseism. Figure 5(c) illustrates the correlation of windiness and the 1.7Hz seism, occurring with no appreciable delay.

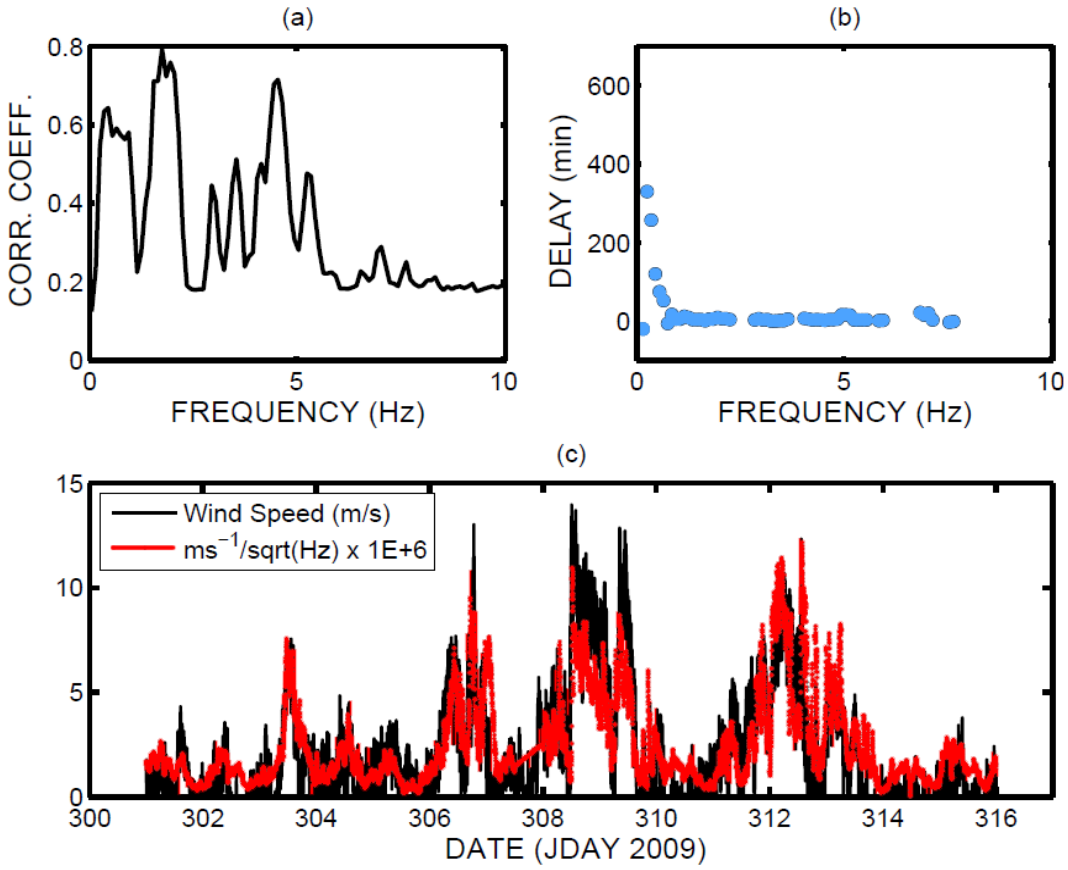

Figure 5 – Correlation between the spectral amplitude of seismic noise for the N component of motion and the wind speed throughout the duration of our survey. (a) Maxima of the normalized correlation function. (b) Time lags corresponding to the maximum of the correlation function. (c) Comparison between the times series of wind velocity (black) and seismic noise spectral density at the frequency 1.7Hz (red).

3.2 Measurement in the near field

The time-frequency plot in Figure 6 depicts one turbine activation sequence. Soil motion data are recorded in close proximity of the turbine. In the composite spectrum we observe the onset of persistent components at peculiar frequencies. Among these we note: (i) some gliding spectral peaks at multiples of 0.3 Hz up to frequencies of 20Hz; (ii) a few steady spectral peaks, the most energetic of which at about 0.45Hz and 1.7Hz. The turbine is 3-bladed. We thus hypothesize that the observed 0.3Hz-spaced gliding spectral peaks are due to structure vibrations associated with the rotor movement, which at the time of measurements had a noted period of about 10s. The time stationarity of the 0.45Hz and 1.7Hz peaks indicates they might be associated to mechanical modes of the turbine structure itself.

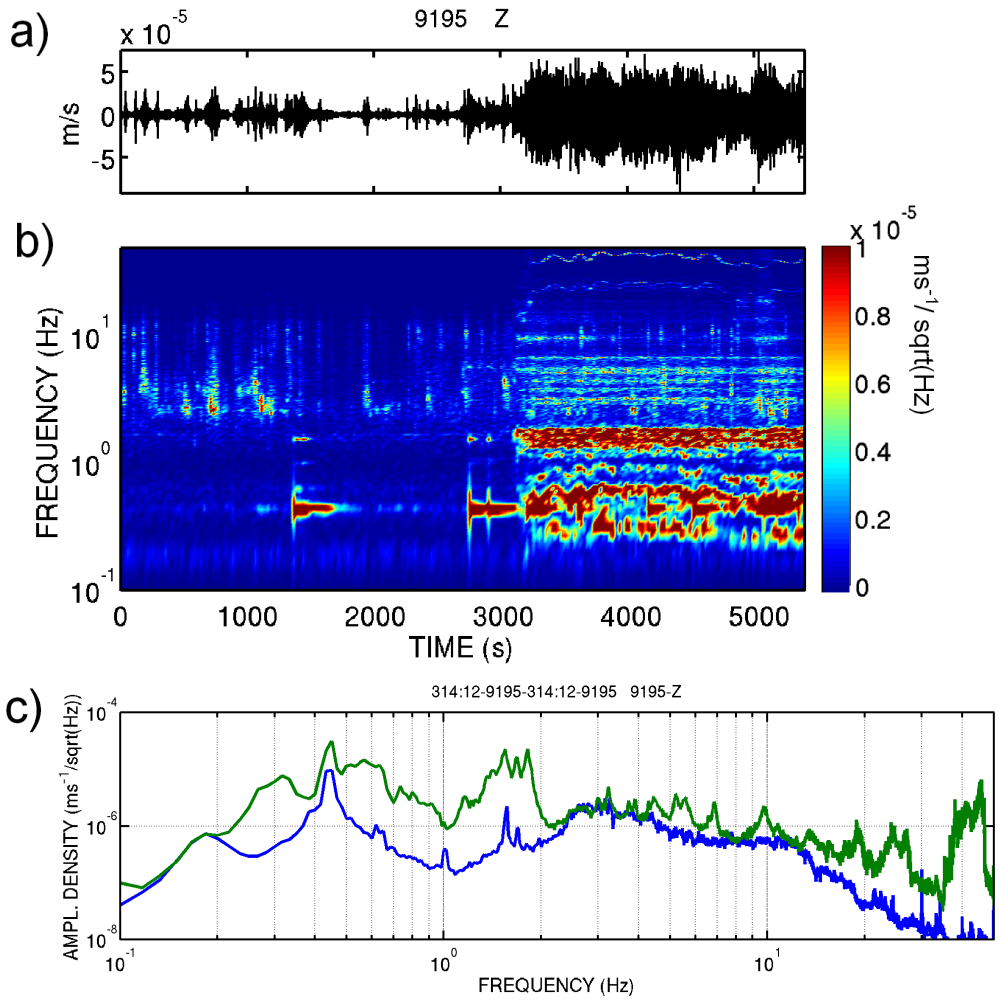

Figure 6 – (a) Measure of the Z component of the ground velocity and (b) related spectrogram measured close to turbine n.2. Data were recorded on Nov.10 during a period of low winds (3m/s).The turbine switched on at about second 3100th. (c) The bottom plot compares velocity spectrum close to the turbine when the WT was off (blue) and active (green).

3.3 Measurement of directional properties

Kinematic properties (velocity and direction of propagation) of the seismic wave-field are measured with dense arrays (sensors spacing of ~100m) deployed in proximity of the wind park (see inset in Figure 7). Data are analyzed with the PWF method (*Plane Wave Fitting*, [Del Pezzo, 11]). In the approximation of plane wave fronts, this method estimates the two components of the slowness vector using the inter-station delays corresponding to the maximum of the cross-correlation function.

We note (Figure 7) an abrupt variation of wave-field direction and velocity around 1Hz. Below 1Hz the wave field direction is consistent with a source located in proximity of the coast, thus reinforcing the hypothesis it is the microseism wave-field associated to marine activity, which has been thoroughly investigated at Virgo also in other studies [Acernese, 12]. Above 1Hz the wave field direction is consistent with a source located in proximity of the wind park (red lines in Figure 7, right). Additional wave-field properties, as its polarization which indicates a prevalence of a transverse wave (see [8]) and the low velocity (0.1-0.2 km/s), suggest that the seismic signal propagates mainly as a Love wave type. Measured properties indeed agree with those typically observed for shear waves in not-consolidated sediments [Castagna, 13].

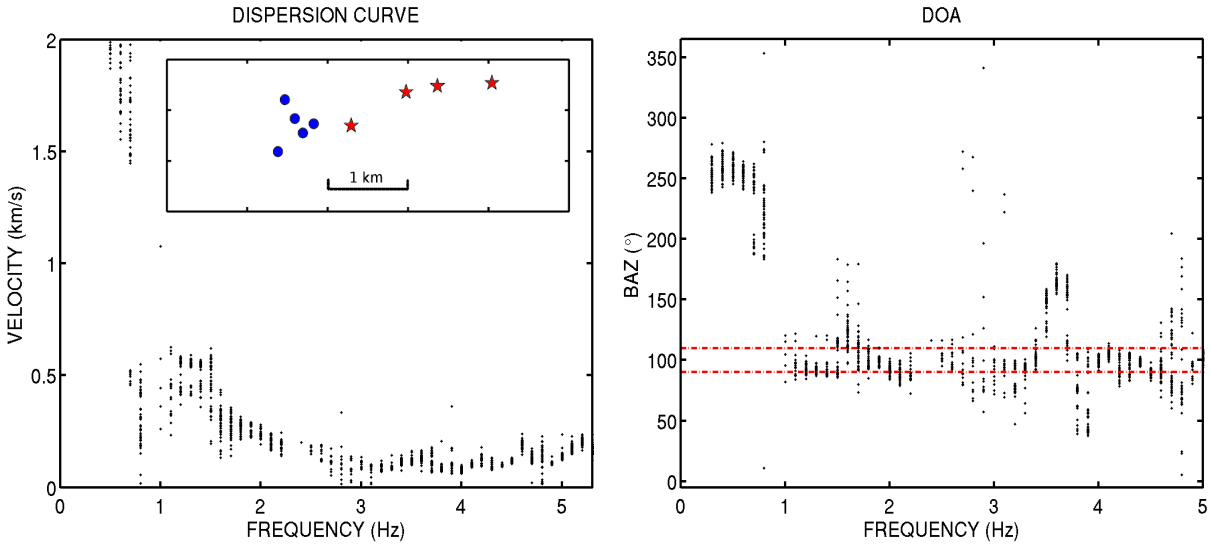

Figure 7 – (Left) Dispersion curves derived from the frequency dependent slowness estimate. Slowness data are obtained from 24 consecutive not overlapping 600s long segments. The inset shows the configuration of the array used for the slowness estimate (blue circles) with respect to the wind park (red stars). (Right) Wave back-azimuth (direction of arrival) as function of frequency. Two dashed red lines mark the angular interval encompassing the wind park.

4. Attenuation properties of WT seismic field and its model

In Figure 8 the seismic field spectral amplitude is compared among synchronized stations located at increasing distance, 1.2km to 11km, from the wind park barycenter. The measurement was done during a windy night for which we expect low anthropic noise and large radiation from the wind park.

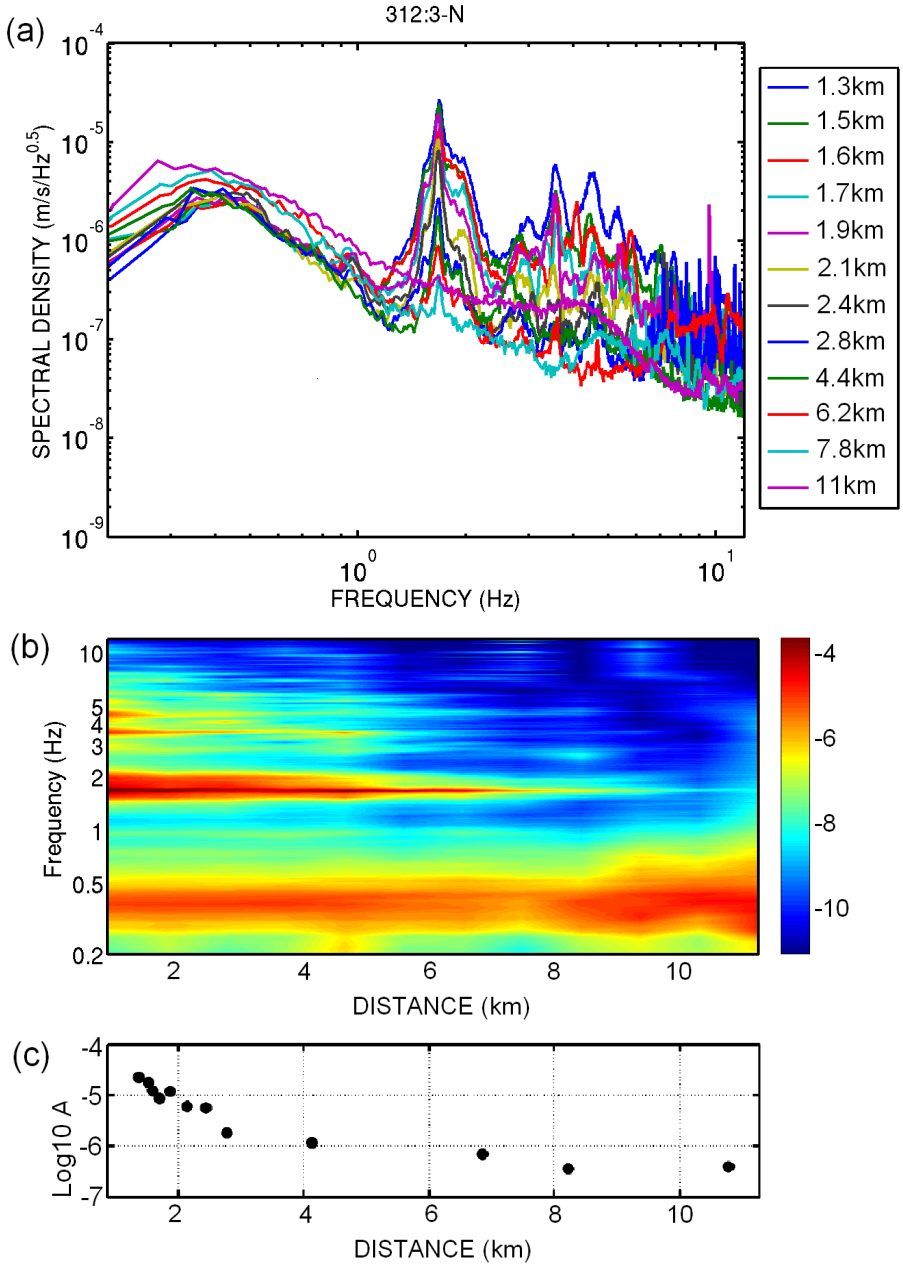

Figure 8 – (a) Amplitude spectral density of ground seism (North-South component) at increasing distances from the wind park. Data are recorded during a windy night period (average wind speed of 14m/s). (b) The logarithm of spectral amplitude (units of $ms^{-1}/\sqrt{Hz}$) is plotted as a function of frequency and distance from the wind park barycenter. (c) Spatial decay of the amplitude of the 1.7Hz peak.

As shown by means of overlapped amplitude spectra and an intensity map (Figure 8,a and Figure 8,b) seismic noise peaks attenuate as receding from the wind park, in agreement with the hypothesis that they are originated by the turbines. A bit surprisingly, the 1.7Hz component appears to travel the farther distance being still distinguishable at a distance of 11km from the park (seismic station inside the Virgo west building). The 1.7Hz seismic component exhibits a complicate attenuation pattern with distance (Figure 8,c). In particular, we observe a marked change in the amplitude decay rate at a source–receiver distance of 2500-3000m.

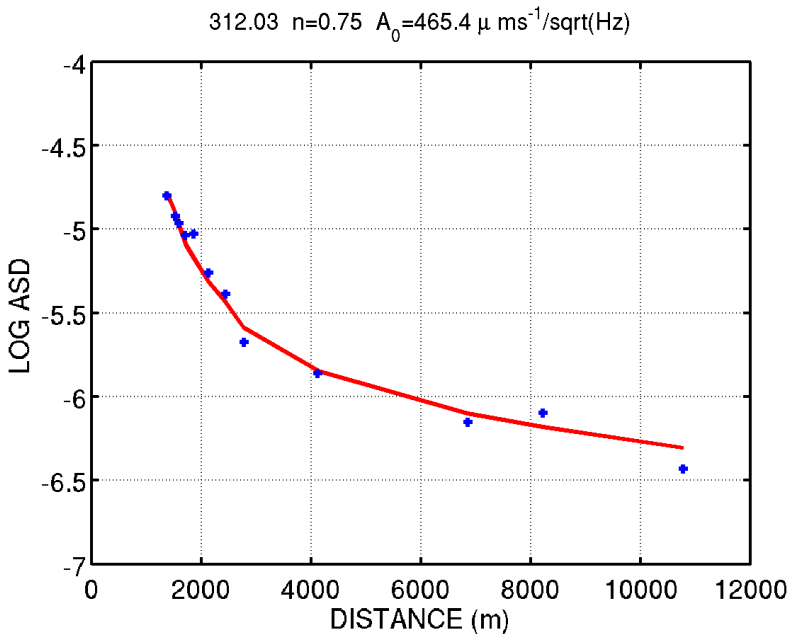

Figure 9 – Spatial decay of the Amplitude Spectral Density of ground velocity computed over a 0.1Hz bin encompassing the 1.7Hz frequency, as function of distance from the wind park barycenter. Blue dots are experimental data. In red is the fit curve using the described model, with parameters: n=0.75, A_0=465μms^{-1}/√Hz.

We can explain the two different decay rates using a simple model accounting for the site geology. We hypothesize that the observed signal is the result of the superposition of direct surface waves and body waves refracted at the 800m-deep carbonate layer. We also assume that the velocity structure of the propagation medium is homogeneous and local amplification effects are negligible. Figure 10 illustrates the model.

It is assumed that each turbine emits energy isotropically, half of it as a surface wave travelling with group velocity v_0 within the shallow layer of quality factor Q_0 and half of it as a body wave travelling through an intermediate layer (Q_1, v_1) and continuously refracted at the interface with a deeper and more rigid layer (Q_2, v_2). The laws describing the attenuation with distance of the two seismic wave components (direct A_D, and refracted A_R) of a single turbine are (Eq.1 and Eq.2):

(Eq.1) $$A_D(f,r) = \frac{A_0}{\sqrt{r}} e^{\frac{-\pi f r}{Q_0 v_0}}$$

(Eq.2) $$A_R(f,r) = A_0(2r_1 + r_2)^{-n} e^{\frac{-2\pi f r_1}{Q_1 v_1} - \frac{-\pi f r_2}{Q_2 v_2}}$$

Assuming *N* identical turbines which signals sum constructively ([1]), the total seismic field at the receiver, located at distances r_i *(i =1…N)* from the individual turbines, is given by (Eq.3):

(Eq.3) $$A_T(f) = A_0 \sum_{i=1}^{N} (A_D(f,r_i) + A_R(f,r_i))$$

A minimization procedure is applied to fit the model to the measured data letting the free parameters (A_0, n, Q_x and v_x, $x=0,1,2$) to span over a defined grid of sensible values. The "Q_x" and "v_x" fit values are consistent with the rounded values given in Figure 10 and with the typical values reported in literature [Campbell, 14] for a soil with the geological characteristics of the study area. The best estimate (one sigma C.L.) of the other parameters is: n=0.70±0.04 and A_0=400±26$\mu ms^{-1}/\sqrt{Hz}$, where the A_0 value corresponds to an average wind speed of 14m/s measured 10m high from soil.

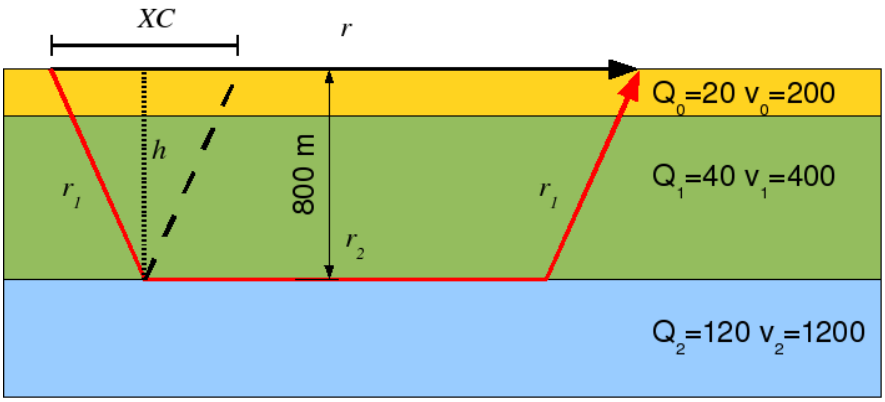

Figure 10 – Sketch of the model of propagation of the seismic wave-field between one WT source located at the left top and a receiver at surface distance "r" at the top right. Direct waves (black arrow) are confined in the shallow layer (yellow), while body waves (red arrow) cross an intermediate layer (green) and are continuously refracted by the 800m deep carbonate layer (blue). The critical distance (XC) is defined by the critical angle of refraction between the intermediate and the carbonate layers: $XC=2h \cdot \tan(\sin^{-1}(v_1/v_2))$. Consequently, for a source located at the surface, refracted waves can be observed only at distances larger than XC. Reported wave speeds (v_x) and quality factors (Q_x) are representative values for the site geology.

[1] This is a working hypothesis. A more realistic estimate shall consider that turbines are not all in phase neither all emit at exactly the same frequency. In this case, the sum law in Eq.3 shall be replaced by a quadratic sum.

5. Predictive relationship applied to the wind park extension

We still have to include in the model the effects of wind. The correlation between seismic noise amplitude and wind speed can be tentatively evaluated considering that the power in the seismic signal shall be proportional to the power that the turbine extracts from the wind. This last is proportional to the cube of the air velocity ([2]). It seems therefore reasonable to expect the seismic noise amplitude (square root of the seismic noise energy) to grow as the 3/2 power of the wind speed.

Figure 11 shows the correlation between the amplitude of the seismic signal at 1.7Hz measured through the entire seismic campaign at the reference station (931E) and the wind velocity measured at Virgo (10m from soil). Although data are a bit dispersed (and we would attribute this mainly to differences in the wind field between Virgo and the wind park) they are sufficiently well described by the model (*W* is wind speed) in Eq.4:

(Eq.4) $$A_{REF}(W) = c + a \cdot W^{\frac{3}{2}}.$$

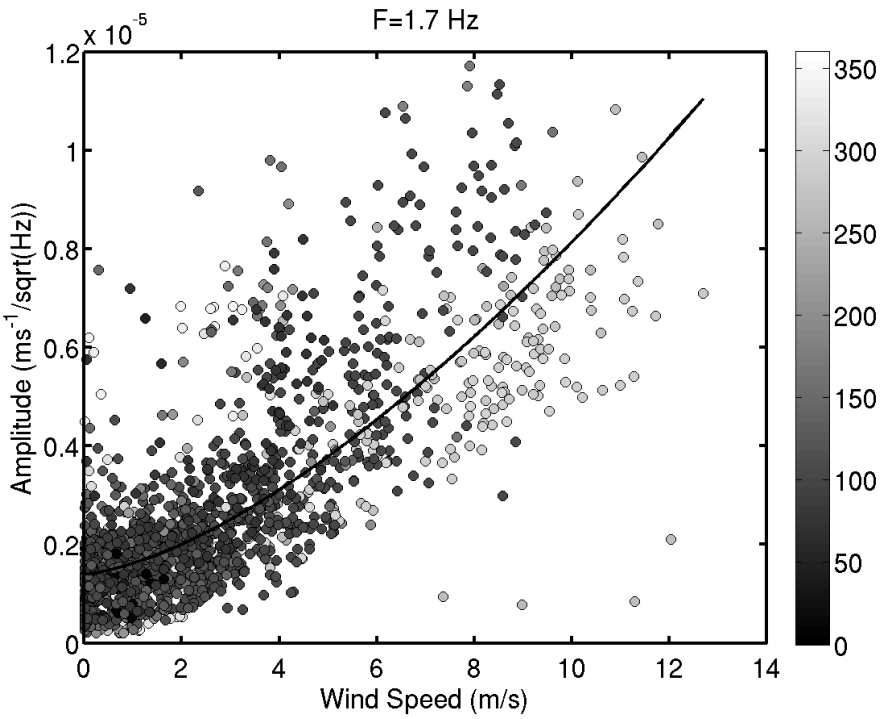

Figure 11 – Scatter plot of the amplitude spectral density at 1.7Hz measured at 931E and the wind speed through the whole seismic campaign period (i.e. about three weeks).The grey-tones scale indicates the wind direction (degrees) measured clockwise from North. The black curve is the model: $A_{REF}=c+a\cdot W^{3/2}$ with best fit parameters $c=1.4\times10^{-6}$ $ms^{-1}/\sqrt{Hz}$ and $a=2.1\times10^{-7}/\sqrt{Hz}$.

[2] The power that a turbine extracts from the wind is proportional to the energy of the volume of air flowing through its blades in the unit time. This air volume increases linearly with wind speed, and its energy is proportional to the average air speed squared.

Keeping in mind the mentioned assumptions and limitations, and in presence of a robust wind statistics, the described model permits to predict the soil noise level at any given distance from any given custom configuration of wind turbines on the site.

Figure 12(left) illustrates the model prediction of the increase of seismic noise consequent to the installation of three additional turbines next to the existing “Eolico Gello” wind park. For distances greater than about 2500m, soil vibration at 1.7Hz would become about 1.8 times larger than at present.

We have applied the previsional model also to the new “Guasticce” 6-turbines park. In this case, given the collected wind speed statistics, the model has been used to estimate the probability distribution of the noise seismic amplitude produced by the wind park at increasing distances from it. This is illustrated in Figure 12(right). For example, at Virgo West Building (5000m from the “Guasticce” park), there would be a 95% probability to observe soil displacements smaller than 0.2 μm/√Hz or, vice-versa, a 5% probability to observe soil displacements larger than 0.2 μm/√Hz, produced by the action of the new wind park. These evaluations, together with the spectrum of the typical ground displacement at the Virgo site (Figure 2, left) will permit to set constraints on the minimal desirable distance for the wind park, and suggest changes in the layout or number of turbines.

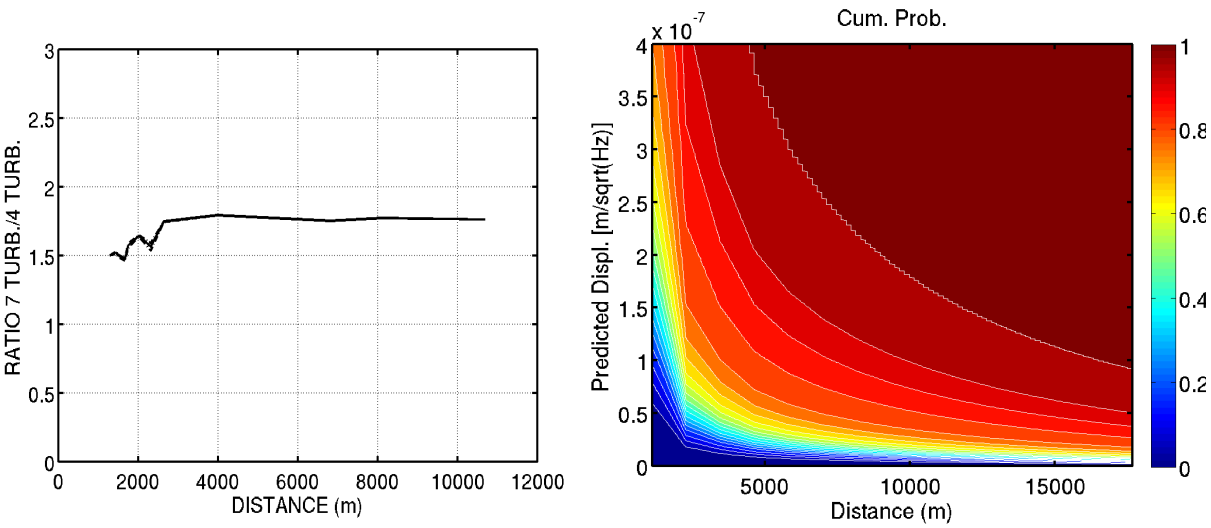

Figure 12 – Examples of application of the previsional model to the proposed new wind turbines in the study area. (Left) Application to the case of the extension of the existing “Eolico Gello” wind park from 4 to 7 turbines: the curve shows the expected increase of ground seism amplitude at 1.7Hz as a function of the distance from the park barycenter. (Right) Application to the case of the proposed “Guasticce” wind park: for any distance from the park barycenter (horizontal axis), the color scale gives the probability that the ground seism amplitude at 1.7Hz produced by the park is less than a given value (selected along the vertical axis). The Virgo West Building is located at 5000m along this distance scale.

6. Conclusions

Experiments which perform high precision measurements require particular attention towards preserving the site seismic climate against potential noise sources. This motivates the interest in evaluating the noise effects of wind turbines. This is indeed the case for the Virgo experiment. The seismic study described in the previous pages has reached two important goals: (1) to measure the main characteristics of the seismic wave-field produced by wind turbines at the Virgo site, and (2) to formulate a model which, with some simplification hypotheses and disposing of a robust wind speed statistics, allows to estimate the increase of ground seismic noise produced by any proposed geometry of wind turbines at the Virgo's sensible receptors.

The study evidenced a low frequency seismic wave-field which, also on the basis of its directional properties and its strong correlation with wind speed, is certainly attributed to the four existing aerogenerators. The most energetic wave-field component is at 1.7Hz and it has the characteristics of a surface shear Love wave with group velocity of 0.2km/s. Quite surprisingly this component is detected, in favorable conditions of wind and low anthropic noise, at epicentral distances of 11km. This poor attenuation is explained accounting for the contribution of a body wave component totally reflected at the interface with the deep carbonate bedrocks layer. We also measure that the wave amplitude correlates with the 3/2 power of the wind speed. The previsional model is built merging these two pieces of information.

On the basis of these results and relying on the use of the previsional model, the EGO consortium has started a negotiation with the local authorities which is aimed to agree on constraints to preserve the site seismic climate.

EGO has also initiated an exchange of information with the "Eolico Gello" managing company. Although, obeying an agreement with the company we cannot make public the turbines data, we can mention that studies concern: (i) switch off tests of the turbines which definitively confirm the origin of the noise; (ii) identification of the 1.7Hz frequency as a structural mode of the tower; (iii) correlation of wind speed data measured at the turbines which help to precise and essentially confirm the result of Eq.4. These studies are still ongoing. In particular, the correlation study of the seismic noise data with turbines operation data might provide hints for reducing the noise emissions.

References

[1] Saulson P R (1994) Fundamentals of Gravitational Waves Detectors, World Scientific, Singapore, 316pp.

[2] Cantini P, Testa G, Zanchetta G and Cavallini R (2001) The Plio-Pleistocene evolution of extensional tectonics in northern Tuscany, as constrained by new gravimetric data from the Montecarlo basin (lower Arno valley, Italy). Tectonophysics 330, 2543.

[3] Stefanelli P, Carmisciano C, Caratori Tontini F, Cocchi L, Beverini N, Fidecaro F and Embriacon D (2008) Microgravity vertical gradient measurement in the site of Virgo interferometric antenna (Pisa plain, Italy). *Annals of Geoph.* 51, 877-886.

[4] The Virgo collaboration (1997) Virgo Final Design Report, code VIR-TRE-DIR-1000-13 available at https://pub3.ego-gw.it/itf/tds.

[5] Accadia T et al. (2010) The seismic Super Attenuators of the Virgo gravitational waves interferometer, Proc. 14th Int. Meeting on Low Frequency Noise and Vibration and its Control, Aalborg, Denmark 9 – 11 June 2010.

[6] Accadia T et al. (2009) Noise from scattered light in Virgo's second science run data. *Class. Quantum Grav.* 27, 194011.

[7] Schofield R (2001) Seismic Measurements at the Stateline Wind Project. LIGO T02010400Z.

[8] Styles P, Stimpson I, Toon S, England R and Wright M (2005) A Detailed Study of the Propagation and Modelling of the Effects of Low Frequency Seismic Vibration and Infrasound from Wind Turbines. Proc. 1st International Meeting on Wind Turbine Noise: Perspectives for Control, Berlin 17-18 October 2005.

[9] Fiori I, Giordano L, Hild S, Losurdo G, Marchetti E, Mayer G, and Paoletti F (2009) A study of the seismic disturbance produced by the wind park near the gravitational wave detector GEO600. Proc. 3rd Int. Meeting on Wind Turbine Noise, Aalborg, Denmark, 17-19 June 2009.

[10] Saccorotti G, Piccinini D, Cauchie L and Fiori I (2011) Seismic Noise by Wind Farms: A Case Study from the Virgo Gravitational Wave Observatory Italy. *Bull. Seism. Soc. Amer.* 101, 2, doi: 10.1785/0120100203.

[11] Del Pezzo E and Giudicepietro F (2002) Plane wave fitting method for a plane, small aperture short period seismic array: a MATHCAD 2000 professional program. Computer and Geosciences 28, 59-64.

[12] Acernese F et al. (2004) Properties of seismic noise at the Virgo site. *Class. Quantum Grav*. 21, S433-S440.

[13] Castagna J P, Batzle M L and Eastwood R L (1985) Relationships between compressional-wave and shear-wave velocities in clastic silicate rocks. *Geophysics* 50, 4, 571-581.

[14] Campbell K W (2009) Estimates of Shear-Wave Q and K0 for Unconsolidated and Semi-consolidated Sediments in Eastern North America. *Bull. Seism. Soc. Amer*. 99, 4, 2365-2392.